Research Papers

Precise nondestructive location of defective woody tissue in grapevines affected by wood diseases

Ana Teresa VAZ[1], Giovanni DEL FRARI[1,*], Ricardo CHAGAS[1], António FERREIRA[2], Helena OLIVEIRA[1], Ricardo BOAVIDA FERREIRA[1]

[1] *LEAF, Instituto Superior de Agronomia, Universidade de Lisboa, 1349-017 Lisboa, Portugal*
[2] *Faculdade de Medicina Veterinária, Avenida da Universidade Técnica, Universidade de Lisboa, 1300-477 Lisboa, Portugal*
*Corresponding author. E-mail: gdelfrari@isa.ulisboa.pt

Summary. Grapevine trunk diseases are major threats to viticulture. A diverse array of Ascomycetes and Basidiomycetes can affect perennial and, indirectly, annual organs of grapevines. Early infections produce wood discolouration, brown wood streaking, black spots and wood necroses. However, all wood symptoms are internal, making nondestructive identification of infected plant material very difficult. To date, there are no nondestructive methods for detecting the presence of developing wood infections, neither in nursery nor field conditions. This means that infected propagation material is planted into new vineyards. Three technologies, magnetic resonance imaging (MRI), computed tomography scan (CT scan) and X-Ray microtomography (Micro-CT), were assessed for determining presence, location and extent of grapevine wood defects caused by fungal infections. Results indicated that MRI lacked resolution to differentiate between asymptomatic and defective wood. CT scan analyses revealed substantial differences in radiodensity when comparing asymptomatic wood to wood with black spots, necroses, and decay. Greatest resolution was achieved with micro-CT (6 μm). This technology precisely distinguished asymptomatic from defective wood, for wood symptoms including necrosis, decay, black spots and brown wood streaking affecting individual xylem vessels, in perennial wood and canes. Micro-CT was thus the best method for nondestructive identification of wood defects resulting from infections. Further work is required to make this technology feasible for the rapid screening of grapevine nursery stock, both in nurseries and at planting.

Keywords. CT scan, micro-CT, MRI, grapevine trunk diseases.

INTRODUCTION

Nondestructive techniques have been increasingly used to observe and characterize the interior of trees, logs, fruit and vegetables, and other living organisms (Ruiz-Altisent *et al.*, 2010). These techniques are often applied in wood industries, in forestry and urban trees. Examples include the identifi-

cation of decayed woody tissues, the presence of which increases the risk of tree failure in urban areas, study of the health status of valuable tree specimens, and the commercial value of standing timber trees or industrial logs. The aim of these methods is to differentiate asymptomatic wood from defective necrotic or decayed wood (Bucur, 2003b; Nicolotti *et al.*, 2003; Bucur, 2005; Baietto *et al.*, 2010; Bieker and Rust, 2010). These methods also assist studies of anatomy and of some physiological processes in woody plants (Brodersen, 2013; Wang *et al.*, 2013; Choat *et al.*, 2016). The most popular nondestructive techniques include ultrasound-based analyses (Nicolotti *et al.*, 2003; Bucur, 2005), magnetic resonance imaging (Pearce *et al.*, 1997; Clearwater and Clark, 2003), and X-Ray-based techniques, such as computed tomography scan (CT scan) and X-Ray microtomography (micro-CT) (Lindgren, 1991; Bucur, 2003a; Milien *et al.*, 2012; Earles *et al.*, 2018).

Nondestructive techniques may assist detection and study of grapevine trunk diseases (GTDs). Grapevines (*Vitis vinifera* L.) affected by GTDs exhibit reduced vigour, productivity and overall life span, contributing to heavy economic losses (Hofstetter *et al.*, 2012). Infected vines have internal symptoms for months to years before the appearance of visible external symptoms, on leaves, berries and shoots (Bertsch *et al.*, 2013). Early internal wood symptoms are brown streaking, black spots, necrosis and decay. Several studies have attributed the former three symptoms to the action of different Ascomycetes, while wood decay, most often white rot, is the result of Basidiomycete infections (Surico *et al.*, 2008; Bertsch *et al.*, 2013; Fontaine *et al.*, 2016; Gramaje *et al.*, 2018). Within the esca complex, one of the most threatening GTDs, the Ascomycetes involved are *Phaeomoniella chlamydospora* and *Phaeoacremonium* spp., while *Neofusicoccum parvum*, *Lasiodiplodia theobromae*, and other *Botryosphaeriaceae* are associated with the syndrome Botryosphaeria dieback. *Phomopsis viticola* causes Phomopsis cane blight, and *Eutypa lata* and other *Diatrypaceae* cause Eutypa dieback. The pathogenicity of these fungi has been proven in controlled studies (Sparapano *et al.*, 2000a; Savocchia *et al.*, 2007; Úrbez-Torres *et al.*, 2013). Under field conditions, however, several of these pathogens are often found simultaneously in symptomatic plants (Bruez *et al.*, 2016; Del Frari *et al.*, 2019). Among the Basidiomycetes, members of genera *Fomitiporella*, *Inonotus*, *Inocutis*, *Stereum* and *Fomitiporia* have been isolated in plants affected by wood decay (Gramaje *et al.*, 2018), with *F. mediterranea* being a primary pathogen (Sparapano *et al.*, 2000b).

Current GTDs control strategies are often unreliable, offering only partial protection of grapevines (Mondel-

lo *et al.*, 2018). Therefore, non-destructive detection of wood defects in infected grapevines would benefit nurseries, by minimizing the production of contaminated nursery stock. Vines with defective wood could be treated (e.g. endotherapy; Del Frari *et al.*, 2018) or discarded to prevent disease spread to newly established vineyards. The present research compared the nondestructive technologies magnetic resonance imaging, computed tomography scan, and X-Ray microtomography for assessing presence, location and extent of wood defects in grapevines.

MATERIALS AND METHODS

Sampling of vineyards for asymptomatic and symptomatic wood, and pathogen identification

One-year-old grapevine canes, young and adult grapevines (*Vitis vinifera* L.) of cultivars Cabernet-Sauvignon, Trincadeira, Touriga Nacional and Castelão, located in the experimental vineyards of the Instituto Superior de Agronomia, Lisbon, were collected in 2010, 2011 and 2017 for the different analyses. The two vineyards, Almotivo and Vinha Velha, had planting densities of 3,333 plants ha^{-1}, the soil was a vertisoil, and the vineyards were managed under conventional practices without irrigation. The Almotivo vineyard was planted in 1998 with cv. Trincadeira, Touriga Nacional and Cabernet-Sauvignon, grafted on 140 RU rootstocks. The vineyard had a history of esca, exclusively manifest in cv. Cabernet-Sauvignon, with approx. 1% of vines showing tiger stripe symptoms on leaves. The Vinha Velha vineyard, which hosted cv. Castelão, was uprooted during the study (2010) as it was heavily affected by GTDs. The prevalent symptoms observed during the two years prior to uprooting were apoplexy, black-dead arm, and greater than 20% plant incidence of tiger stripe foliar symptoms.

Sampling occurred as follows. For cv. Castelão, numerous plants were examined for the presence of GTD internal symptoms at the tops and bases of the trunks, during the vineyard uprooting, and ten symptomatic trunks were selected. For cv. Trincadeira and Touriga Nacional, six plants per cultivar were randomly selected and uprooted, and the trunks were stored for further examination. For cv. Cabernet-Sauvignon, six trunks and 20 1-year-old canes were randomly sampled and cut into 30 cm segments before storage. All sampled wood material was stored at 4°C until further processing.

Fungi were isolated from symptomatic wood, and its proximities, by cutting wood into small pieces (approx. 3 mm^3), then sterilizing them by flaming, followed by immersion in a NaClO solution (0.05% w/w

active chlorine) for 1 min, and double rinsing in sterile distilled water. Surface-sterilized wood was dried on sterile filter paper and placed on Petri dishes (90 mm diam.) each containing 15 mL of potato dextrose agar (BD-Difco Laboratories) supplemented with 250 mg L^{-1} chloramphenicol (BioChemica). The Petri dishes were then incubated at 25 ± 1°C, in the dark, for 21 d. Colonies emerging from the wood were identified based on morphological and cultural features (macro- and microscopic analyses of mycelium, conidia and conidiomata), revealing the presence of the ascomycete *Phaeomoniella chlamydospora* and other wood *Botryosphaeriaceae* pathogens. The Basidiomycete *Fomitiporia* sp. was consistently isolated from decayed wood, which was a white-rot type of decay. In a separate study, conducted on cv. Cabernet-Sauvignon plants, numerous wood pathogens, including *Phaeomoniella chlamydospora*, *Fomitiporia* sp., *Fomitiporella* sp., *Neofusicoccum* spp., *Diaporthe* sp. and *Eutypa* spp., were identified using DNA metabarcoding (Del Frari *et al.*, 2019).

Nondestructive identification of wood defects

The nondestructive identification of brown wood streaking and black spots, wood defects associated with brown wood streaking of rooted cuttings and Petri disease (Surico 2009), esca, and other GTDs, was the prime objective of this study. However, symptoms of necrosis and white rot were frequently observed, so the following four categories were defined for symptoms identification:

(i) *Early stages of infection.* Presence of brown wood streaking and/or black spots (Figure 1A);
(ii) *Advanced stages of infection.* Presence of symptoms described in (i), and central or sectorial necroses of different size (Figure 1B and C);
(iii) *White rot stage.* Presence of white rot, defined as 'a soft, friable, spongy mass' (wood decay; Mugnai *et al.*, 1999), which, in the present study, always occurred in plants exhibiting advanced stages of infection (Figure 1D);
(iv) *Asymptomatic wood.* Absence of all of the symptoms described in categories (i), (ii), and (iii) (Figure 4A).

Trunks and canes were scanned using the methods outlined below and, afterwards, they were manually sectioned to confirm the presence and locations of the symptoms.

Magnetic resonance imaging (MRI)

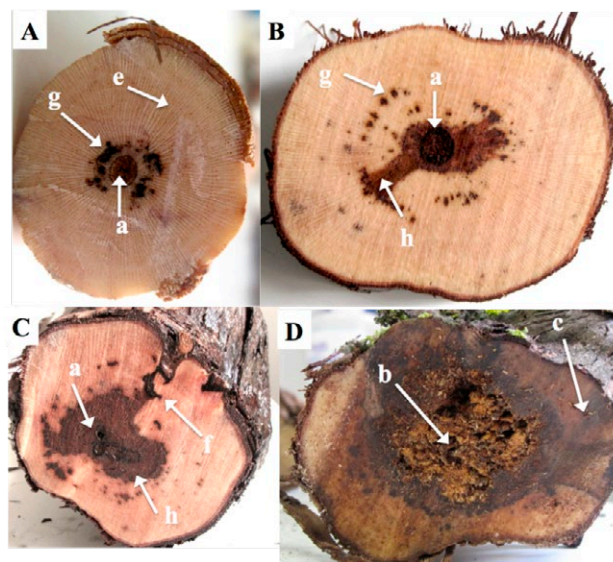Measurements were performed in a medical laboratory (Laboratório de Radiologia, Alverca, Portugal), using

Figure 1. Cross-sections of grapevine trunks of different ages showing wood defects. (A) Early stages of wood infection, (B) and (C) advanced stages of infection, and (D) trunk affected by white rot. (a) Pith and holes, (b) decayed wood, (c) extended wood necrosis, (e) asymptomatic wood, (f) wood knots, (g) black spots, (h) central necrosis. Lower case letters represent some of the features identified in Table 1.
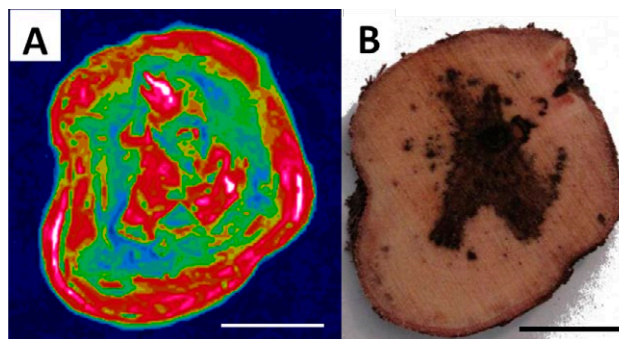

Figure 2. Magnetic resonance image (A) and the corresponding original photograph (B) of a grapevine trunk (cv. Castelão). Scale bars = 1 cm.

an Aris Elite, manufactured by Hitachi. This instrument employs 4-channel RF system with QD MER coil, and scalable Dual-Quad RF receiver system and support for RAPID parallel imaging. The instrument was equipped with self-shielded vertical permanent magnet of Tesla strength = 0.3 T. The gradient system characteristics were slew rate = 55 T m^{-1} sec^{-1} and amplitude = 21 mT m^{-1}. Three grapevine trunk samples (approx. length 20 cm, diam. = 3 cm) were scanned, and ten transversal slices per sample were recorded (slice thickness, SL =

3.0 mm). Spin echo imaging used repetition time (TR) = 4000 ms, and echo time (TE) = 80 ms. The image matrix was 256 × 256 pixels with a field of view (FOV) = 42 cm. Image processing was carried out with Hitachi dedicated software. Trunks of grapevine cv. Castelão were analysed using MRI (n = 3).

Computed tomography scan (CT scan)

CT scan is based on the attenuation of X-Rays by a sample, due to differences in its density, water content and chemical composition (Lindgren, 1991). A medical TOMOSCAN AV CT Philips scanner was used with the following CT scan settings: acceleration voltage = 120 kV, and exposure time + 2 s at 90 mA. Scans were made in radial cross-section, using optic slices of wood 270 mm × 5 mm. The reconstruction matrix of the resulting images was 512 × 512 pixels. The measured X-Ray intensity was converted into grey scale, in which darker regions represented low densities and bright regions high densities. The attenuation values calculated for each pixel were translated into grey scale or colour scale, and transformed into an image of the cross-sections of the samples. For medical scanners, the radiodensity, expressed in Hounsfield units (H), is -1000 H for air (0 kg m^{-3}), 0 H for water (1000 kg m^{-3}) and +1000 H for human bone. The scans were saved in DICOM format and viewed and analysed using Osirix v.3.7.1 32-bit software. Trunks of grapevine cv. Trincadeira and Touriga Nacional were analysed using CT-scan (n = 4).

X-Ray microtomography (micro-CT)

When compared to pre-existing X-Ray methods (including CT scan), the major difference of micro-CT is the scanning of objects from different radial positions, resulting in a series of different projections that are mathematically transformed and combined using appropriate algorithms. Each resulting tomogram is an image of known size and coordinates of each pixel. The combination of multiple tomograms along the axial vector of the object yields a full 3-dimensional representation. The different attenuations were quantified in Hounsfield units and, for visualization, they are expressed by grey values for each pixel. Grapevine trunks and 1-year-old canes were examined by this technique using a SkyScan 1174 compact micro-CT (courtesy of SkyScan, Kontich, Belgium, and Dias de Sousa SA, Lisbon, Portugal), and related SkyScan software to process the images. Trunks and canes of cv. Cabernet-Sauvignon vines were analysed using micro-CT (trunks, n = 4; canes, n = 10).

RESULTS

Magnetic resonance imaging

MRI failed to give enough resolution to accurately differentiate between asymptomatic and defective wood. The comparison between one MRI image of a sample with advanced stages of infection (Figure 3A) and the photograph of the corresponding section (Figure 3B) revealed no clear distinction between regions of defective and asymptomatic tissues, especially for brown streaking and black spots. Figure 3A shows that the high-intensity signal regions corresponded to affected areas as well as asymptomatic areas of woody tissue. The black spots visible in Figure 3B were not identified, in Figure 3A, as high-intensity signal areas.

Computed tomography scan (CT scan)

Visualization of the cross-sectional images obtained from the CT scanner and the analysis of the resulting tomographic reconstructions revealed clear differences between asymptomatic and defective wood areas, which were imputable to density alterations induced by fungal infections (Figure 3). Image contrast was defined as the signal intensity difference detected among different types of tissues.

Analysis of samples at different stages of wood infection revealed variations in radiodensity values, according to the various anatomical and symptom features (Table 1). Selected CT images were compared with the original photographed sections illustrating early (A1) and advanced (A2) stages of infection, as well as the white rot stage (A3) (Figure 3). When observing the grey-scale images (Figure 3B), dark shades indicated regions of low radiodensity, whereas bright areas indicated material of greater radiodensity. Comparisons between the original photographs and the corresponding tomography images showed that black spots, and to a lesser extent necrotic wood, presented brighter shades than asymptomatic wood, which was due to greater radiodensity (Hounsfield Units, H) of the diseased areas (Table 1; Figure 3). An alternative colour scale (UCLA colour scale, Osirix v. 3.7.1; Figure 3C) aided differentiation of black spots from necrotic wood tissue and other areas. In the section A3 of Figure 3, the cross-section shows (i) internal necrotic wood, exhibiting high radiodensity, (ii) sectorial necrosis, and (iii) wood decay. Sectorial necrosis and wood decay were regions of low radiodensity, due to absence of water and the transformation of woody tissue in response to the action of Basidiomycetes, and were visualized as dark-coloured areas in Figure 3 B3.
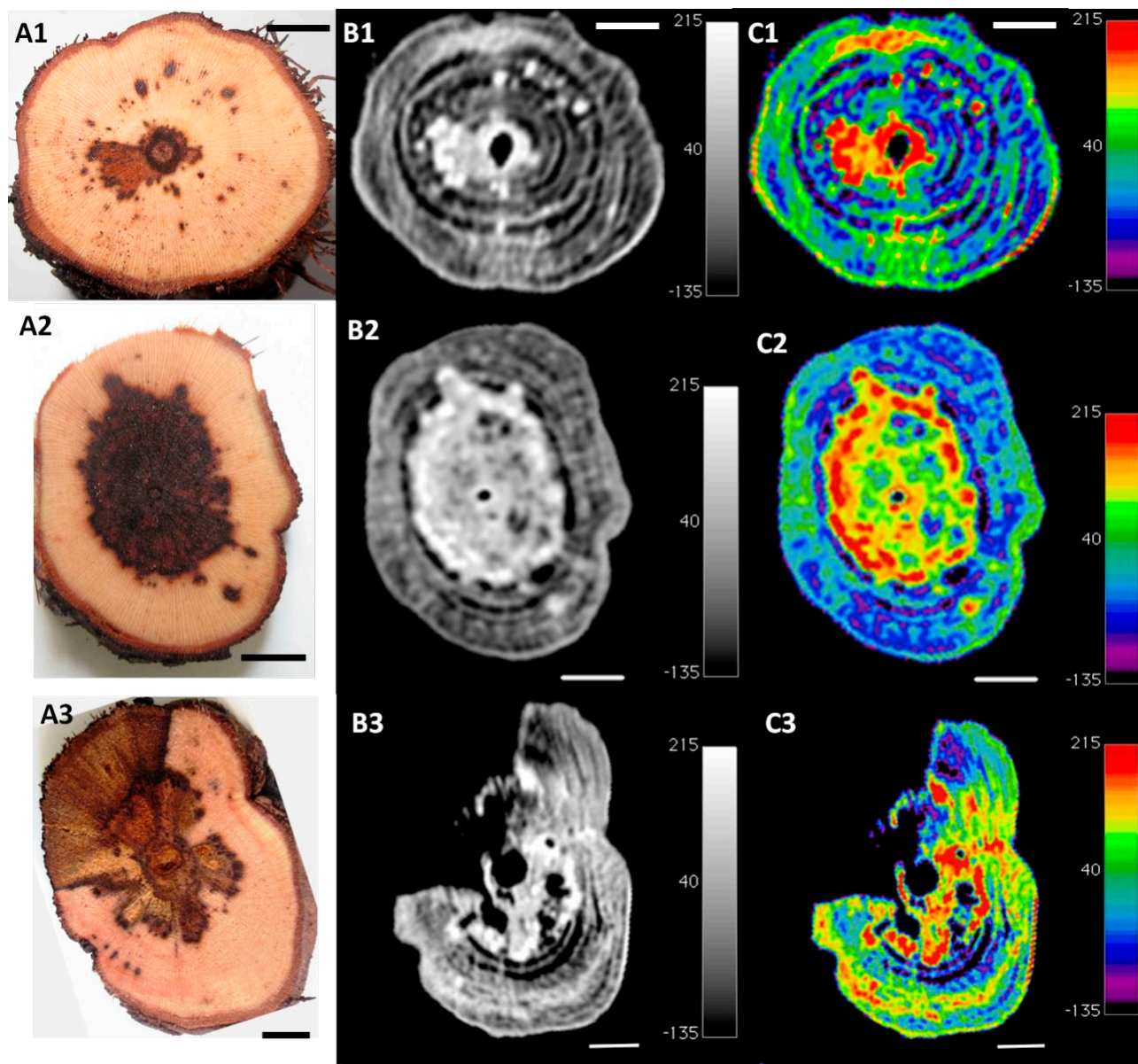
Figure 3. Original photographs (A) and computed tomography scan images (B and C) showing a symptomatic grapevine trunk (cv. Touriga Nacional) at (1) early, and (2) advanced stages of infection, and (3) white rot stage. (B) Tomographic analysis (grey colours; and (C) tomographic analysis (UCLA colours), according to the radiodensity scales presented on the right side of B and C. Scale bars = 1 cm. CT scan images extracted from Osirix v. 3.7.1.

X-Y plots extracted from Osirix v.1.3.7.v. (Figure 4) show three examples of variation (H) along cross-sections of asymptomatic wood (A), early stage of infection (B) and white rot stage (C). In asymptomatic vines, radiodensity values varied between -40 ± 47 H for empty xylem vessels and +76 ± 27 H for asymptomatic wood (Table 1; Figure 4A). During early stages of infection (Figure 4B), the radiodensities of the two black spots (g) in the section corresponded to +251 H and +264 H

(from left to right). Overall, the pith and holes, as well as decayed wood and other necrotic tissue affected by Basidiomycetes, exhibited reduced radiodensity, ranging from approx. -900 H to -300 H. For example, during the white rot stage (Figure 4C), sectorial necrosis (c) gave radiodensity of -439 H and wood decay (b) of -760 H, revealing low density of these tissues. The wood transformed by the action of decay agents (e.g. *F. mediterranea*) had low water and high air contents, which
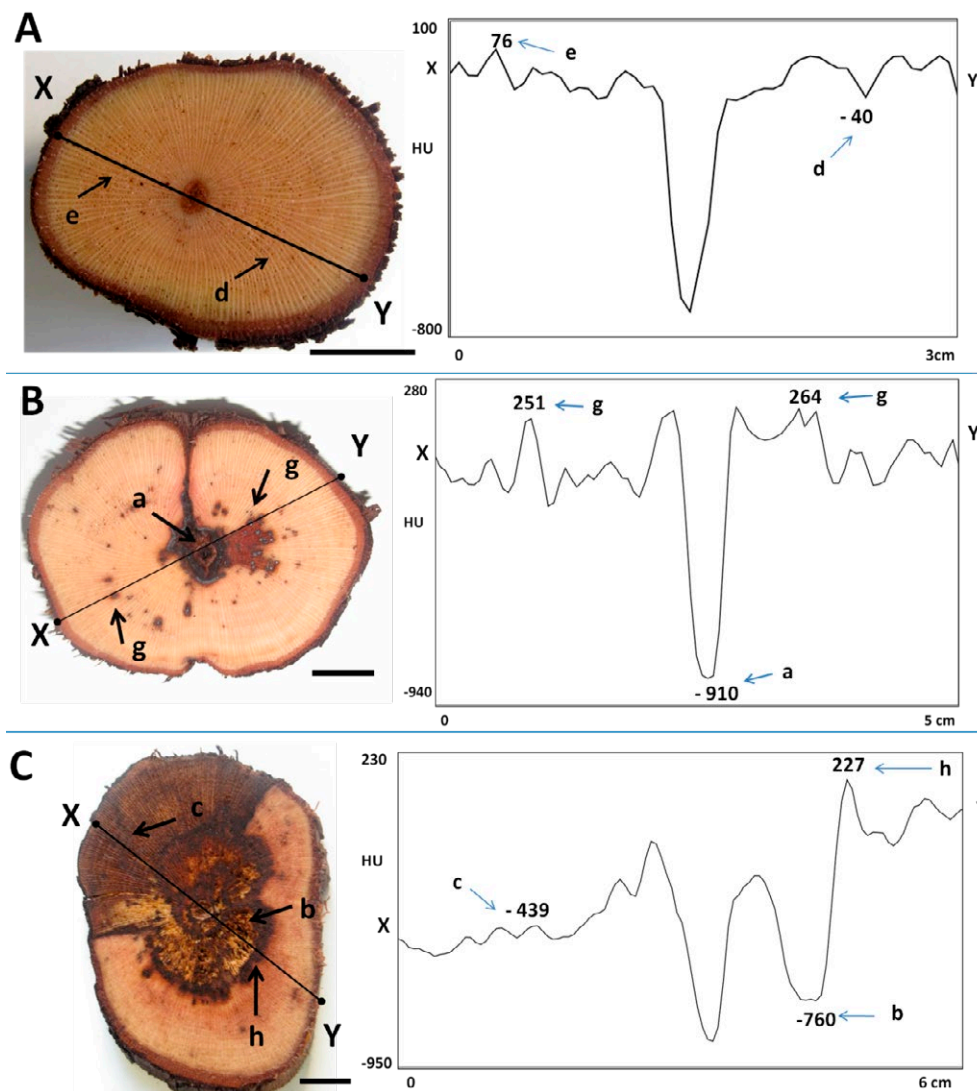
Figure 4. Grapevine trunk sections (cv. Trincadeira) and the corresponding X-Y plots, showing patterns of radiodensity variation across the lines indicated, in different areas of infection. (A) Asymptomatic grapevine, (B) early stage of infection and (C) white rot stage. Scale bars = 1 cm. X-Y plots extracted from OsiriX Viewer v.3.7.1. Lower case letters represent the features identified in Figure 1 and Table 1.

translated into low radiodensity CT images. The X-Y plot also shows an area of wood with high radiodensity, corresponding to necrotic wood (h), at +227 H (Figure 4C; Table 1), hypothetically not yet affected by decay.

X-Ray microtomography (micro-CT)

While CT scan gave promising results for black spot detection, as well as necrosis and wood decay, accurate identification of brown wood streaking was not attained. For this reason, micro-CT was assessed, as a technique capable of achieving greater resolution. Figure 5 shows micro-CT detection of high-density material (white

colour) inside individual xylem vessels of a grapevine trunk (cv. Cabernet Sauvignon). On the cross-section (Figure 5A), the clear presence of xylem vessels partially or completely filled with gums was confirmed by visual inspection/photography after slicing the grapevine trunk (not shown). A longitudinal section of the same trunk is shown in Figure 5B, illustrating discontinuity of gums along the trunk xylem vessels.

One-year-old canes were also examined using this technique. In this case, high resolution images were acquired (6 μm), confirming the results presented above. To achieve rapid screening, fundamental for application of this technique in large-scale environments (e.g. nurs-

Table 1. Radiodensity values (H) obtained from computerized axial tomography for distinct parts of grapevine wood, either asymptomatic or with different wood defects. Lower case letters represent the features identified in Figures 1 and 4. Mean ± standard deviation (n = 40 wood sections, 4 grapevine trunks).

Feature	Radiodensity (Hounsfield Units, H) Mean +/- SD
Pith and hole (a)	-860 ± 55
Wood decay (b)	-700 ± 70
Extended central/sectorial necrosis (c)*	-430 ± 94
Empty vessels (d)	-40 ± 47
Asymptomatic wood (e)	+76 ± 27
Knots (f)	+204 ± 54
Black spots (g)	+234 ± 56
Early necrotic wood (h)	+264 ± 68

*in plants at white rot stage

eries), lower resolution (25 μm) images were acquired, such as that shown in Figure 6. This resolution achieved with micro-CT gave the possibility of identifying individual xylem vessels in the early stages of symptom expression, namely brown wood streaking.

Other non-invasive techniques tested by the authors of this study lacked the required levels of sensitivity to non-destructively detect symptoms of grapevine wood infection. Among them, there were techniques based on ultrasounds, Fourier transform infrared spectroscopy (FTIR), particle/proton-induced X-Ray emission (PIXE), electrical impedance spectroscopy (EIS) and radiography.

DISCUSSION

This study tested three nondestructive techniques for assessing the presence of fungus-induced wood
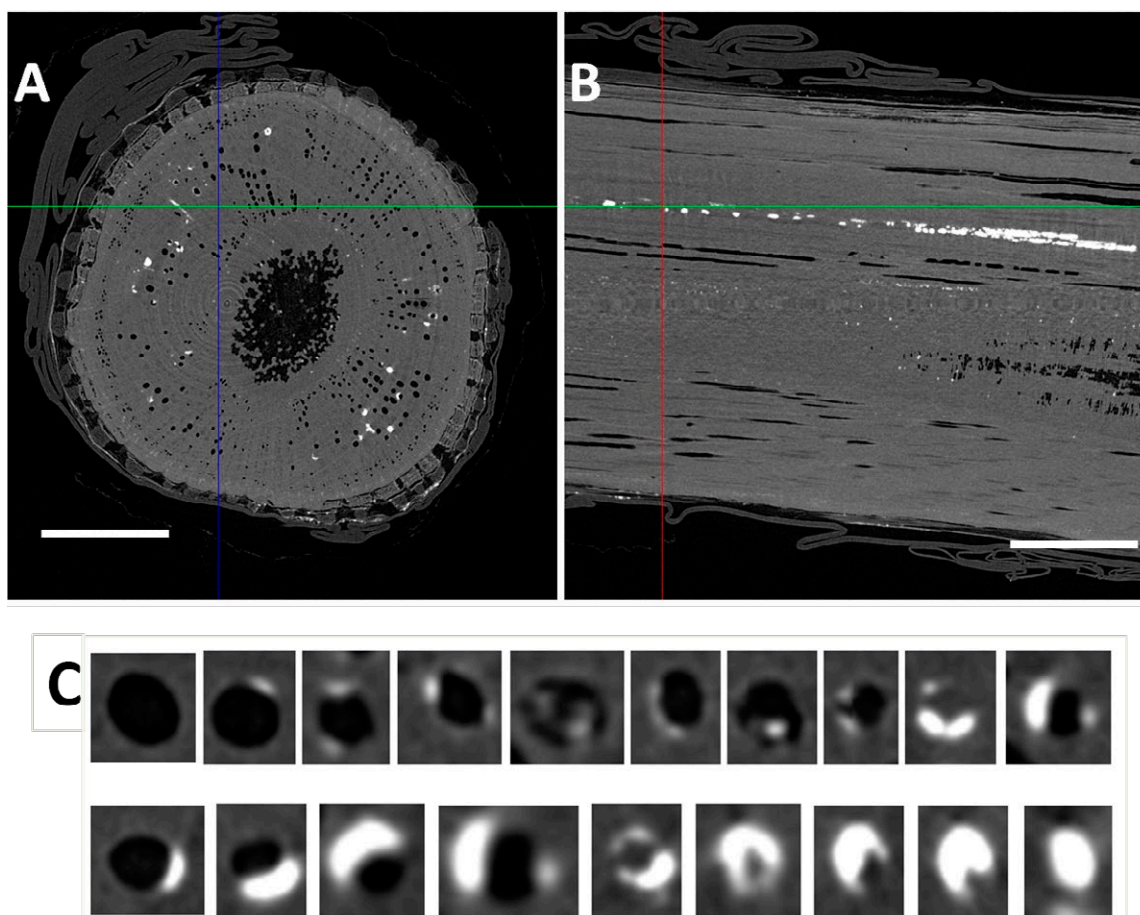

Figure 5. X-Ray microtomography (micro-CT) of a grapevine trunk (cv. Cabernet Sauvignon) infected by wood pathogens. (A) Cross-section showing some vessels partially or completely filled with gums. (B) Corresponding longitudinal section showing the accumulation of high-density material along the xylem vessels. (C) Individual xylem vessels with increasing gum accumulation in each from empty (top left) to filled (bottom right). Scale bars = 1 cm, resolution 6 μm.
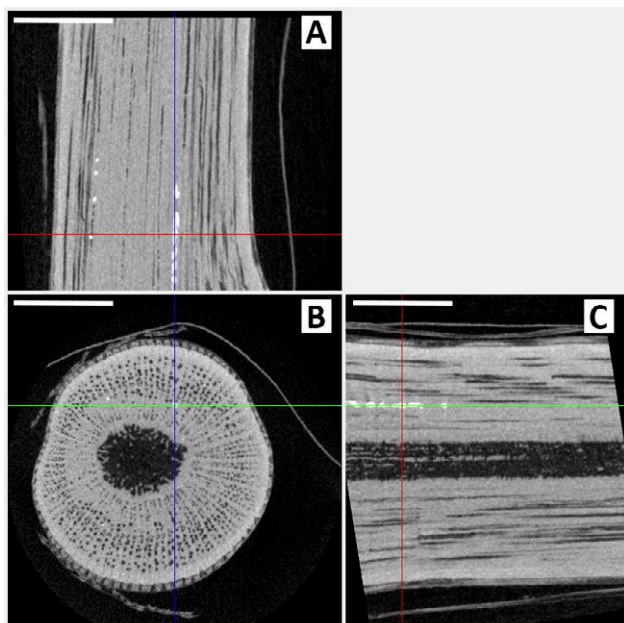
Figure 6. X-Ray microtomography (micro-CT) of a 1-year-old cane of cv. Cabernet Sauvignon. (A and C) Longitudinal sections, and (B) cross-section, with horizontal and vertical lines pinpointing individual xylem vessel(s) filled with gums. Scale bars = 5 mm, resolution 25 μm.

defects in grapevine trunk and stem tissues. CT scan and micro-CT were effective for detecting the presence of early and advanced stages of infection. Both methods detected black spots, wood necrosis and wood affected by the action of basidiomycetes (wood decay). In addition, micro-CT detected the earliest symptoms of wood infection, namely the appearance of brown wood streaking in individual xylem vessels. This highlights the potential of micro-CT for application in nursery environments. Despite these promising results, some wood defects (e.g. brown streaking) are not exclusively the results of a fungus infection, but may also be caused by other factors such as mechanical injuries. Furthermore, under some circumstances wood pathogens may occur in asymptomatic wood (Del Frari et al., 2019).

MRI has been frequently used to locate fungal decays or cavitation in trees (Müller et al., 2001; Bucur, 2003a), or to follow the development of core breakdown disorder in pear fruit (Lammertyn et al., 2003). Kuroda et al. (2006) showed that magnetic resonance micro-images can measure water distribution and areas affected by pathogenic microorganisms in living tree stems, but small vessels (20 to 30 μm diam.) filled with water could not be visualized. These authors found a theoretical resolution of 117 μm, in the best analyzed situation, which allowed the identification of xylem vessel aggre-

gates, despite not being sensitive enough to pinpoint individual vessels (Kuroda et al., 2006). These observations are similar to those of the present study (Figure 2). Under our experimental conditions and with the instrument used, MRI did not reveal defective wood. However, other studies that employed high-resolution MRI (e.g. 7.05 Tesla, 1.0 T m^{-1}) in grapevines, were successful in detecting individual xylem vessels, for example in examination of water ascent in embolized xylem vessels (Wang et al., 2013) and water-stress induced cavitation (Choat et al., 2010). Therefore, MRI has potential to be exploited in the detection of defective wood. Further studies could also assess the contribution of secondary metabolites to MRI signals (Oven et al., 2008). From the practical viewpoint, a portable MRI was developed and tested in 2012 in living trees, but the low level of resolution only allowed analysis of water content in mature trees and wood (Jones et al., 2012). Nevertheless, a patent concerning a portable MRI system was recently granted (US9910115B2), increasing possibilities for the development of a prototype capable of increased resolution and applicability in vineyards.

Both X-Ray techniques used in the present study (CT scan and micro-CT) enabled clear imaging of wood defects in grapevines, at different stages of infection. When comparing these two techniques, micro-CT allowed more precise analysis of symptoms in grapevine wood, due to the increased resolution of the equipment, when compared to CT scan. A resolution of approx. 6 μm is achieved by using micro-CT, which, after translation into high-quality images, allowed rigorous identification of individual xylem vessels that were entirely or partially filled with gums. As far as the authors are aware, there is no other technology that allows non-invasive and nondestructive detection of these symptoms in vines affected by wood pathogens.

Successful applications of CT scanning in woody tissues include accurate and nondestructive measurements of wood density (Funt and Bryant, 1987; Lindgren, 1991) in plants affected by fungal diseases (Okochi et al., 2007), and examination of the water distribution in stems of living trees (Habermehl et al., 1990; Fromm et al., 2001). Our results support this understanding, showing that the action of wood pathogens alters wood composition, either by increasing (e.g. black spots) or decreasing wood density (e.g. wood decay; Figure 4), when compared to asymptomatic woody tissue, resulting in different radiodensity signals. The major limitation of CT scan is the typical size of the instruments, which prevents application under field conditions.

As postulated, micro-CT was the best technology for accurate identification of presence, extent and precise

location of wood defects in grapevines (Figure 5). Recent studies have shown similar results, in grapevines, where micro-CT was successfully applied to characterize wood anatomy (Milien *et al.*, 2012; Brodersen, 2013), infection by the Botryosphaeria dieback pathogen *Neofusicoccum parvum* (Czemmel *et al.*, 2015), and other physiological processes, such as xylem vessel dehydration and refilling (Choat *et al.*, 2016; Brodersen *et al.*, 2018), and estimation of starch content (Earles *et al.*, 2018). Despite these promising results, to find a robust application of micro-CT in large-scale environments (e.g. nurseries), it is necessary to optimize scanning parameters (e.g. reducing resolution to increase scanning speed), and portability, always allowing for the potential hazards caused by radiation.

CONCLUSIONS

Early nondestructive detection of wood defects caused by grapevine wood pathogens represents an important step towards controlling these serious threats for grape production. No chemical treatment is capable of eradicating wood pathogens from infected wood. Successful *in vitro* efficacy of fungicides often did not translate to *in vivo* efficacy, so research has shifted to nurseries and pruning wound protection, as an integrated GTDs management strategy (Gramaje *et al.*, 2018; Mondello *et al.*, 2018). While investigating new chemicals and ways to deliver them to infected tissues, some of the technologies assessed in the present study could have short and medium term practical applications. In the short term, X-Ray-based scanning techniques could be implemented in nurseries, screening propagation material for internal GTDs symptoms and allowing removal of symptomatic individuals. This may reduce market inputs of infected plant material. In the medium term, when effective chemical treatments become available, this technology could be applied in the field, to find and treat young plants during early stages of infection. A patent application based on the results shown in this study was recently granted in the European Union, the United States and other countries (PCT/EP2011/068320). Future investigations will focus, therefore, on improving the portability, speed and efficiency of these techniques, as well as the search for new treatments to control *in vivo* wood pathogens.

ACKNOWLEDGEMENTS

LITERATURE CITED

Baietto M., Wilson A.D., Bassi D., Ferrini F., 2010. Evaluation of three electronic noses for detecting incipient wood decay. *Sensors* 10: 1062-1092. DOI: 10.3390/s100201062.

Bertsch C., Ramírez-Suero M., Magnin-Robert M., Larignon P., Chong J., … Fontaine F., 2013. Grapevine trunk diseases: complex and still poorly understood. *Plant Pathology* 62(2): 243–265. DOI: 10.1111/j.1365-3059.2012.02674.x.

Bieker D., Rust S., 2010. Non-destructive estimation of sapwood and heartwood width in scots pine (*Pinus Sylvestris* L.). *Silva Fennica* 44(2): 267–273.

Brodersen C.R., 2013. Visualizing wood anatomy in three dimensions with high-resolution X-Ray micro-tomography (MCT) – a review. *IAWA Journal* 34(4): 408–424. DOI: 10.1163/22941932-00000033.

Brodersen C.R., Knipfer T., McElrone A.J., 2018. *In vivo* visualization of the final stages of xylem vessel refilling in grapevine (*Vitis vinifera*) stems. *New Phytologist* 217: 117–26. DOI: 10.1111/nph.14811.

Bruez E., Baumgartner K., Bastien S., Travadon R., Guérin-Dubrana L., Rey P., 2016. Various fungal communities colonise the functional wood tissues of old grapevines externally free from grapevine trunk disease symptoms. *Australian Journal of Grape and Wine Research* 22: 288–295

Bucur V., 2003a. Nondestructive characterization and imaging of wood. Springer-Verlag, Berlin, Heidelberg. DOI: 10.1007/978-3-662-08986-6.

Bucur V., 2003b. Techniques for high resolution imaging of wood structure: a review. *Measurement Science and Technology* 14(12): R91-R98. DOI: 10.1088/0957-0233/14/12/R01.

Bucur V., 2005. Ultrasonic techniques for nondestructive testing of standing trees. *Ultrasonics* 43 (4): 237–39. DOI: 10.1016/j.ultras.2004.06.008.

Choat B., Drayton W.M., Brodersen C., Matthews M.A., Shackel K.A., … McElrone A.J., 2010. Measurement of vulnerability to water stress-induced cavitation in grapevine: a comparison of four techniques applied to a long-vesseled species. *Plant, Cell and*

Environment 33: 1502–1512. DOI: 10.1111/j.1365-3040.2010.02160.x.

Choat B., Badel E., Burlett R., Delzon S., Cochard H., Jansen S., 2016. Noninvasive measurement of vulnerability to drought-induced embolism by X-Ray microtomography. *Plant Physiology* 170 (January): 273–282. DOI: 10.1104/pp.15.00732.

Clearwater M.J., Clark C.J., 2003. *In vivo* magnetic resonance imaging of xylem vessel contents in woody lianas. *Plant, Cell and Environment* 26: 1205–14.

Czemmel S., Galarneau E.R., Travadon R., McElrone A.J., Cramer G.R., Baumgartner K., 2015. Genes expressed in grapevine leaves reveal latent wood infection by the fungal pathogen *Neofusicoccum parvum*. *PLoS ONE* 10: e0121828. DOI: 10.1371/journal.pone.0121828

Del Frari G., Costa J., Oliveira H., Boavida Ferreira R., 2018. Endotherapy of infected grapevine cuttings for the control of *Phaeomoniella chlamydospora* and *Phaeoacremonium minimum*. *Phytopathologia Mediterranea* 57(3): 439–48. DOI: 10.14601/Phytopathol_Mediterr-23515.

Del Frari G., Gobbi A., Rønne Aggerbeck M., Oliveira H., Hestbjerg Hansen L., Boavida Ferreira R., 2019. Characterization of the wood mycobiome of *Vitis vinifera* in a vineyard affected by esca. Spatial distribution of fungal communities and their putative relation with leaf symptoms. *Frontiers in Plant Science* 10: 910. DOI: 10.3389/fpls.2019.00910

Earles J.M., Knipfer T., Tixier A., Orozco J., Reyes C., … McElrone A.J., 2018. *In vivo* quantification of plant starch reserves at micrometer resolution using X-Ray microCT imaging and machine learning. *New Phytologist* 218: 1260–1269. DOI: 10.1111/nph.15068.

Fontaine F., Gramaje D., Armengol J., Smart R., Z.A. Nagy, … Corio-Costet M.-F., 2016. Grapevine trunk diseases. A review. OIV publications, 1st Edition: May 2016 (Paris, France), 25 pp. http://www.oiv.int/public/medias/4650/trunk-diseases-oiv-2016.pdf.

Fromm J.H., Sautter I., Matthies D., Kremer J., Schumacher P., Ganter C., 2001. Xylem water content and wood density in spruce and oak trees detected by high-resolution computed tomography. *Plant Physiology* 127: 416–425. DOI: 10.1104/pp.010194

Funt B., Bryant E.C., 1987. Detection of internal log defects by automatic interpretation of computer tomography images. *Forest Products Journal* 37(1): 56–62.

Gramaje D., Urbez-Torres J.R., Sosnowski M.R., 2018. Managing grapevine trunk diseases with respect to etiology and epidemiology: current strategies and future prospects. *Plant Disease* 102(1): 12–39. DOI: 10.1094/PDIS-04-17-0512-FE

Habermehl A., Hüttermann A., Lovas G., Ridder H.W., 1990. Computer-tomographie von bäumen. *Biologie in Unserer Zeit* 20: 193–200.

Habermehl A., Ridder H.W., 1982. Method and apparatus for testing materials such as disease in living trees. https://patents.google.com/patent/CA1138576A/pt.

Hofstetter V., Buyck B., Croll D., Viret O., Couloux A., Gindro K., 2012. What if esca disease of grapevine were not a fungal disease? *Fungal Diversity* 54: 51–67. DOI: 10.1007/s13225-012-0171-z

Jones M., Aptaker P.S., Cox J., Gardiner B.A., McDonald P.J., 2012. A transportable magnetic resonance imaging system for *in situ* measurements of living trees: the tree hugger." *Journal of Magnetic Resonance* 218: 133–140. DOI: 10.1016/j.jmr.2012.02.019

Kuroda K., Kanbara Y., Inoue T., Ogawa A., 2006. Magnetic resonance micro-imaging of xylem sap distribution and necrotic lesions in tree stems. *IAWA Journal* 27: 3–17. DOI: 10.1163/22941932-90000133

Lammertyn J., Dresselaers T., Van Hecke P., Jancsók P., Wevers M., Nicolaï B.M., 2003. MRI and X-Ray CT study of spatial distribution of core breakdown in 'Conference' pears. *Magnetic Resonance Imaging* 21 (7): 805–815. DOI: 10.1016/S0730-725X(03)00105-X

Lindgren L.O., 1991. Medical CAT-Scanning: X-Ray absorption coefficients, CT-numbers and their relation to wood density. *Wood Science and Technology* 25(5): 341–49. DOI: 10.1007/BF00226173

Milien M., Renault-Spilmont A.-S., Jane S., Sarrazin A., Verdeil J.-L., 2012. Visualization of the 3D sructure of the graft union of grapevine using X-Ray tomography. *Scientia Horticulturae* 144: 130–140. DOI: 10.1016/j.scienta.2012.06.045

Mondello V., Songy A., Battiston E., Pinto C., Coppin C., … Fontaine F., 2018. Grapevine trunk diseases: a review of fifteen years of trials for their control with chemicals and biocontrol agents. *Plant Disease* 102(7): 1189–1217. DOI: 10.1094/PDIS-08-17-1181-FE

Mugnai L., Graniti A., Surico G., 1999. Esca (Black Measles) and brown wood-streaking: two old and elusive diseases of grapevines. *Plant Disease* 83: 404–418.

Müller U., Bammer R., Halmschlager E., Stollberger R., Wimmer R., 2001. Detection of fungal wood decay using magnetic resonance Imaging. *Holz Als Roh- Und Werkstoff* 59(3): 190–94. DOI: 10.1007/s001070100202.Nicolotti G., Socco L.V., Martinis R., Godio A., Sambuelli L., 2003. Application and comparison of three tomographic techniques for detection of decay in trees. *Journal of Arboriculture* 29(2): 11.

Okochi T., Hoshino Y., Fujii H., Mitsutani T., 2007. Non-destructive tree-ring measurements for Japanese oak

and Japanese beech using micro-focus X-Ray computed tomography. *Dendrochronologia* 24(2–3): 155–164. DOI: 10.1016/j.dendro.2006.10.010

Oven P., Merela M., Mikac U., Sersa I., 2008. 3D magnetic resonance microscopy of a wounded beech branch. *Holzforschung* 62(3): 322–328. DOI: 10.1515/HF.2008.022

Pearce R.B., Fisher B.J., Carpenter T.A., Hall L.D., 1997. Water distribution in fungal lesions in the wood of sycamore, *Acer pseudoplatanus*, determined gravimetrically and using nuclear magnetic resonance imaging. *New Phytologist* 135: 675–688.

Ruiz-Altisent M., Ruiz-Garcia L., Moreda G.P., Lu R., Hernandez-Sanchez N., … García-Ramos J., 2010. Sensors for product characterization and quality of specialty crops - A review. *Computers and Electronics in Agriculture* 74(2): 176–194. DOI: 10.1016/j.compag.2010.07.002.

Savocchia S., Steel C.C., Stodart B.J., Somers A., 2007. Pathogenicity of *Botryosphaeria* species isolated from declining grapevines in sub tropical regions of Eastern Australia. *Vitis* 46(1): 27–32.

Sparapano L., Bruno G., Ciccarone C., Graniti A., 2000a. Infection of grapevines with some esca-disease associ- ated fungi. II. Interaction among *Fomitiporia punctata*, *Phaeoacremonium chlamydosporum* and *P. aleophilum*. *Phytopathologia Mediterranea* 39: 53–58.

Sparapano L., Bruno G., Ciccarone C., Graniti A., 2000b. Infection of grapevines by some fungi associated with esca. I. *Fomitiporia punctata* as a wood-rot inducer. *Phytopathologia Mediterranea* 39(1): 46–52. DOI: 10.14601/Phytopathol_Mediterr-1542

Surico G., 2009. Towards a redefinition of the diseases within the esca complex of grapevine. *Phytopathologia Mediterranea* 48(1): 5–10.

Surico G., Mugnai L., Marchi G., 2008. The esca disease complex. In *Integrated Management of Diseases Caused by Fungi, Phytoplasma and Bacteria* (Ciancio A., Mukerji K. eds), Springer, Dordrecht, 3: 119–36. DOI: 10.1007/978-1-4020-8571-0_6

Úrbez-Torres J.R., Peduto F., Smith R.J., Gubler W.D., 2013. Phomopsis dieback: a grapevine trunk disease caused by *Phomopsis viticola* in California. *Plant Disease* 97: 1571-1579.

Wang M., Tyree M.T., Wasylishen R.E., 2013. Magnetic resonance imaging of water ascent in embolized xylem vessels of grapevine stem segments. *Canadian Journal of Plant Science* 93: 879–93. DOI: 10.4141/CJPS2013-025